VOL. 11, NO. 11, JUNE 2016 ISSN 1819-6608
ARPN Journal of Engineering and Applied Sciences

www.arpnjournals.com

OPTIMIZATION OF SPIRAL CIRCULAR COILS FOR BIO-IMPLANTABLE MICRO-SYSTEM STIMULATOR AT 6.78 MHz ISM BAND

Mokhalad Khaleel Alghrairi[1], Nasri Bin Sulaiman[1], Roslina Bt Mohd Sidek[1] and Saad Mutashar[2]
[1]Department of Electrical and Electronic Engineering, Faculty of Engineering, University Putra Malaysia UPM Serdang, Selangor Darul Ehsan, Malaysia
[2]Department of Electrical Engineering, University of Technology, Baghdad, Iraq
E-Mail: mokhalad_alghrairi@yahoo.com

ABSTRACT

Unique design of inductive coupling links is very essential in designing batteries bio-implantable devices. This paper, introduce a small size and efficient spiral circular coils (pancake) at 6.78 MHz to be used for bio-implantable devices. A mathematical model for the proposed coil is developed based on the number and width of turns for each coil to determine the outer and internal dimension by summation the width, number of the turns and spacing between them for each coil. The proposed coils are designed using commercial HFSS software. The results shows that the omnidirectional radiation patterns of the proposed coils is constant and stable and can be used for batteries bio-implantable devices.

Keywords: inductive links, bio-implantable devices, coils design, ISM band.

INTRODUCTION

Wireless inductive coupling uses the magnetic field to transfer data and power from the external part to the internal part. Generally, the inductive bio-device system consists of a main coil assimilated and isolated outside the human body which acts as a transmitter antenna and a secondary coil within the body acts as a receiver. Usually, the main coil is tuned in series resonance to provide a low impedance load for driving the transmitter coil, while the secondary coil is parallel almost [1]. Hence, to have better power transfer efficiency of inductive coupling link, both sides of the link are tuned at exactly the same resonant frequency. Also, the distances from the reader coil at the implant device provided by the stability of the RF signal must be highly readable.

Nowadays wireless power transfer for implanted device is more useful than the batteries because of the risks produce from the batteries on body of human like size, chemical effect and the life time that's lead to do surgical process to replace the battery [2]. Currently most of the implanted devices powered transcutaneous using inductive coupling links. The system consisted of two parts, external part to transfer data and power inductively to the internal part (implanted devices) which is located within the body, because of weak links between the two parts the system need efficient design for external and internal coils [3].

Design and optimization of efficient inductive power transmission links have been well studied over the last few decades. By using Ansoft HFSS software, two rectangular coil was designed with external dimension 62 mm × 25 mm and internal 25 mm × 10 mm using 13.56 MHz [4]. This design suffered from size of internal coil and short rang of the coupling distance and details of mathematical derivations to design these coils were not mention. Two spiral square coil with dimension of outer and inner coil as 70 mm × 8 mm and 20 mm × 8 mm by used frequency range (1-5) MHz [5]. This satisfy optimum coupling with distance 10 mm by sweeping the trace width, spacing and the number of turns in an EM simulator.

Another two circular coil design with 38 mm and 36 mm for outer and inner diameter in external and 18 mm and 16 mm for implanted coil respectively was design to get distance between the coil more than 15 mm by used frequency 742KHz [6]. That's lead to take large area inside the tissue. The dimensions of the circular coil's for the coupling links outer and inner transmitters are 56mm and 10mm, respectively, while the receiver coil's coupling links dimensions are 11.6mm and 5mm, respectively. The circuit was designed to operate on a 13.56 MHz frequency, providing a 22mm coupling distance [7]. However, the size of implanted coil still needs to be considered.

Flat spiral circular coils was design for transmitter dimension dout = 12 mm and din = 0 mm and for receiver coil with dimension dout = 11mm and din = 5.25 mm [8]. This design offers optimum coupling links in distance 10 mm, the size and relative short range coupling still need to be considered. However, most of these designs depend on outer and inner diameter respect on number of turns to analyze geometry of coils.

In this paper, the efficient power transmission by design two spiral circular coils with external coil dimension dout = 44 mm and din = 7.92 mm and internal coil dimension dout = 10.5 mm and din = 6.61 mm is presented. The design depend on the number of turn, width turns, space between the turns and length of conductor used in coil by printed on Roger substrate RO4003(tm) to achieve coupling distance 15 mm using industrial specific medical (ISM) operating frequency 6.78MHz.

PLANNER SPIRAL COIL OPTIMIZATION

Applying a magnetic field at the primary coil will induce a current flowing in the secondary. The induced current's value is associated to both the primary and secondary coil's inductors L1 and L2. The following equation (1) calculates the inductance of a chosen circular planar coil as shown in Figure-2 [9].

$$L = \frac{C_1 \mu_0 N^2 d_{avg}}{2}\left[ln\left(\frac{C_2}{\varphi}\right) + C_3\varphi + C_4\varphi^2\right] \quad (1)$$

where N is the no. of turns of the coil, C refers to the coefficient of the circular coil layout based on the values as C1 = 1.00, C2 = 2.46, C3 = 0.00, C4 = 0.20, used from [10].Hence, using equation (1), the coil inductance can be calculated based on the N, fill factor, φ and the arithmetic geometrical mean davrg for each coil.

Equation (1) is used to calculate the self-inductance for each single spiral circular coil, the arithmetic geometrical mean for both the outer and the inner coils. When the turns of the coils are present on the perimeter, similar to filament coils, the fill ratio factor φ, changes to zero. However, it is changed to 1, when the coil turns are spiraled right up to the center. The fill factor is calculated using the Equation (2).

$$\varphi_T = \frac{(d_{out.T} - d_{in.T})}{(d_{out.T} + d_{in.T})} \text{or } \varphi_R = \frac{(d_{out.R} - d_{in.R})}{(d_{out.R} + d_{in.R})} \quad (2)$$

The arithmetic geometrical averages for the external and internal coils should be calculated as given in (3)

$$d_{avg.T} = \frac{(d_{out.T} + d_{in.T})}{2}, \quad d_{avg.R} = \frac{(d_{out.R} + d_{in.R})}{2} \quad (3)$$

The precision of the expression is dependent on the φ and N values, along with S and W, wherein S refers to the space within every turn and W refers to the width of the copper line. In this research, a simple circular coils with easy mathematical models and the internal and the external coil diameters is proposed based on developed Eq. (4)

$$d_{out} = d_{in} + (2N + 1)W + (2N - 1)S \quad (4)$$

To estimate the total parasitic DC resistance for the inductor, the factors that should be estimated are - resistivity of the conductive material, ρc, length of the conductive trace lc, thickness tc, that are described in Table-2 and in the following equation:

$$l_c = \frac{\pi}{2}[2Nd_{in} + \sum_{x=1}^{2N} xW + \sum_{x=1}^{2N-1} xS] \quad (5)$$

$$R_{dc} = \rho_c \frac{l_c}{wt_c} \quad (6)$$

The skin effect will increase the coil AC resistance at higher frequencies and should be taken into account. Considering the skin effect the equivalent series resistance, Rs is given by,

$$\sigma = \sqrt{\frac{\rho_c}{\pi\mu f}} \quad (7)$$

$$R_S = R_{dc} \frac{t_c}{\sigma\left(1 - e^{-\left(\frac{t_c}{\sigma}\right)}\right)} \quad (8)$$

$$\mu = \mu_0\mu_r \quad (9)$$

Where δ is the skin depth, μ0 is the permeability of space, and μr is the relative permeability of the conductor. To design and optimize spiral circular coil (pancake), two concepts were used; the first one is based on (10).

$$d_{out} \leq D2\sqrt{2} \quad (10)$$

In which the radius of the external coil is equivalent to the distance that should be covered (in the case of a smaller internal coil). However, the mutual distance within the outer and the implanted coil is two times the diameter of the embedded coil. The second concept depends on the relation between the external and the internal coil. Thus, the rising mutual distance is recorded by the optimization of the coil dimensions by equating din.T ≈ 0.18; dout.T ≈ din.R ≈ 0.75 dout.R respectively, as published earlier [11]. Based on the above approximations and the chart presented in Fig. 1, that is designed by using an HFSS 15.0 software, the outer coil dimension, dout.T = 44 mm, and din.T =7.92 mm, while the dimensions for the embedded coil were dout.R =10.5 mm, and din.R =6.61 mm, respectively as shown in Table-1.

Table-1. The parameter values of the external and internal coils.

Quantity	Symbol	External coil	Internal coil
Outer diameter	d_{out}	44 mm	10.5 mm
Inner diameter	d_{in}	7.92 mm	6.61 mm
Average diameter	d_{avrg}	25.96 mm	8.55 mm
Mutual Inductance	M	4.5 µH	4.5 µH
Number of turns	N	27	7
Inductor Width	W	0.438 mm	0.14 mm
Turn spacing	S	0.2 mm	0.137 mm
Fill factor	Φ	0.694	0.227
Coupling Coefficient	K	0.105	0.105
Thickness of conductor	tc	0.01mm	0.01mm

Therefore, the outer coil for the optimal design had the dimensions of 7.92 ≈ 0.18 × 44, while the dimensions of the inner coil were nearly 83% of which 6.61 ≈ 0.75 × 10.5%.

In case of two aligned coils, the mutual distance between the transmitter and receiver coils should satisfy the condition in (11)

$$\frac{d_{out.T}}{2} = \sqrt{X^2 + \left(\frac{d_{out.R}}{2}\right)^2} \quad (11)$$

Where, X refers to the distance between both the aligned coils, a and b refer to the radius of the external and the embedded coils, respectively, dout.T and dout.R refer to the exterior and the inside outer dimensions in the case of the transmitter and the receiver coils, as described in Figure-1.

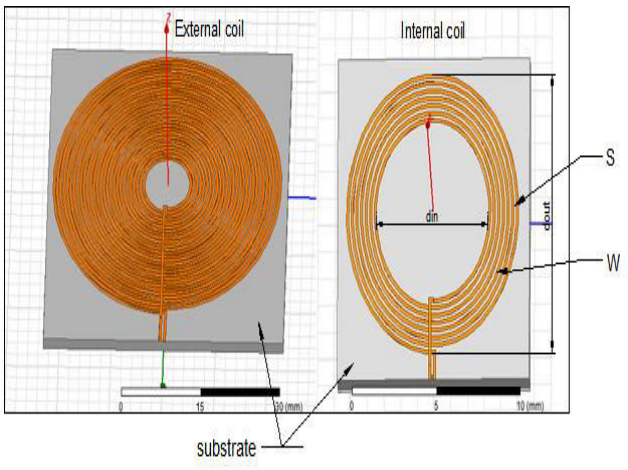

Figure-1. The layout of the printed spiral circular loop coils on a substrate simulate with HFSS.

For the estimation of the mutual inductance of the coils, it should be assumed that both the coils should be aligned and possess parallel circular filaments (Single-turn coils), as illustrated in Figure-2. Both the coils have diameters dT and dR, respectively [12] as illustrated in (12) where; dT and dR refer to the outer dimensions of the transmitter (external) and the receiver (implanted) coils, respectively.

$$M(d_T, d_R, \Delta) = \frac{1}{2}\mu_0\sqrt{d_T \times d_R}\left[\left(\frac{2}{f} - f\right)K(f) - \frac{2}{f}E(f)\right] \quad (12)$$

$$f(d_T, d_R, X) = \left(\frac{4d_T d_R}{(d_T + d_R)^2 + X^2}\right)^{\frac{1}{2}} \quad (13)$$

µo = 4π x 10-9 H/cm represents the permeability of the free space; K and E are the complete elliptic integrals of the first and second kind [13].

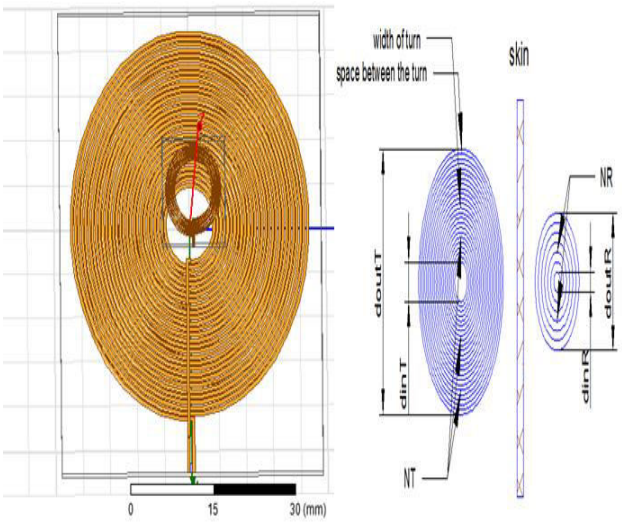

Figure-2. Both coils are aligned and parallel circular filaments.

The complete mutual inductance within both the coils is estimated by summation of the partial mutual inductance within every two coil turns on the pair of the printed spiral coils and is as described below:

$$M_{ij} = G\sum_{i=1}^{n_1}\sum_{j=1}^{n_2} M_{ij}\left(d_{T.i}, d_{R.j}, X\right) \quad (14)$$

where Mij refers to the mutual inductance present between the loop i of the exterior coil and the loop j for the inner coil, G depicts the factor based on the printed spiral shape, wherein, G = 1.0 in the case of a circular shape of the coil [14]. The outer coil contains 27 turns which are separated from each other at a distance of 0.2 mm, and have a width, W=0.438 mm, while the implanted coils have 7 turns and are separated from each other by 0.137 mm, with a width, W=0.14 mm.

Therefore, the approximate mutual inductance within both the spiral circular coils is a function of the coil dimensions, no. of turns for every coil, and the distance, wherein (dout.T ≥ dout.R) [15].

$$M_{T.R} \cong \frac{\mu_0 N_T d_{out.T}^2 N_R d_{out.R}^2 \pi}{2\sqrt{\left(d_{out.R}^2 + X^2\right)^3}} \quad (15)$$

The coupling coefficient, K, between the reader and the implant coil, is based on the coil dimensions and the distance present between both the coils. This coefficient is calculated using the Equation (16).

$$K = \frac{a^2 b^2}{\sqrt{a*b}*(X^2+a^2)^{3/2}} \quad (16)$$

The total efficiency of ηT and ηR can be calculated using Equation (17) which modified from [7]

$$\eta_{total} = \eta_T \eta_R = \frac{k^2 \omega_0^2 L_T L_R^2 R_{load}}{k^2 \omega_0^2 L_T L_R^2 R_{load} + k^2 L_T R_R R_{load}^2 + \omega_0^2 L_R^3 R_T + L_R R_T R_R R_{load}} \quad (17)$$

For developing a better geometric design for the coil using the HFSS software, the coils that are used for the micro-system are those which are on the Rogers RO4003(tm) substrate and have permeability, relative permittivity, and a dielectric loss tangent of 3.55, 1 and 0.0027, respectively based on the thickness of 1.5 mm.

RESULTS AND DISCUSSIONS

The communication bandwidth and link efficiency can be noted that the performance of the inductive coupling link is dependent on the geometry of the coil and includes factors like the size, shape, and the separation tolerance along with the whole size and complexity for the transmitter and the receiver. However, for the geometric coupling link, many factors should be taken into account and have to be calculated, like the mutual distance within the coils (D), the coupling coefficient (K), the mutual inductance (M) and the efficiency (η). Based on the coil dimensions and the Equation (11), it is seen that distance within both the aligned coils is equivalent to 21.36 mm, which is sufficient for the application under research. It can be presented the relation between the proposed dimensions of the coil and the distance in the Figure-3. Based on the equation (16), it is possible to calculate the relation between the distance and the Coupling coefficient (K), which is further observed in Figure-4. In the case of our proposed micro-system design, the distance separating the coils is around 6 mm, thus, the coupling coefficient, K, can be calculated to be 0.105. Moreover, it can calculate the relation between the distance and the mutual inductance (M) using Equation (15), which is further described in the Figure-5.

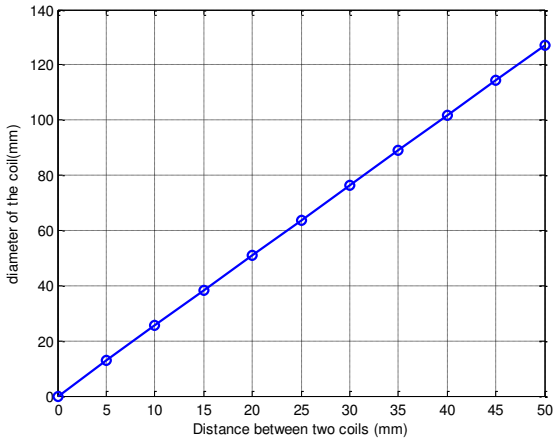

Figure-3. The relationship between the proposed coils dimension and distances.

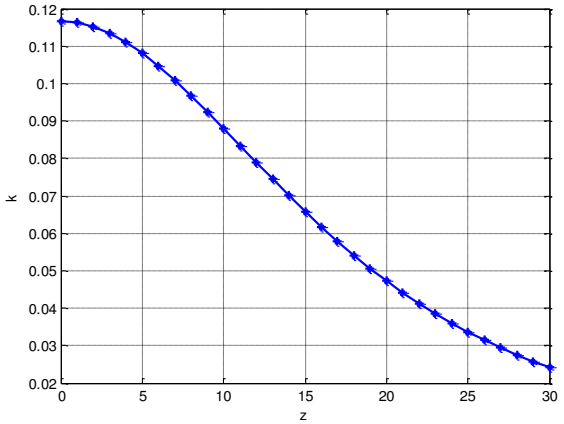

Figure-4. The relationship between distance and coupling coefficient (K).

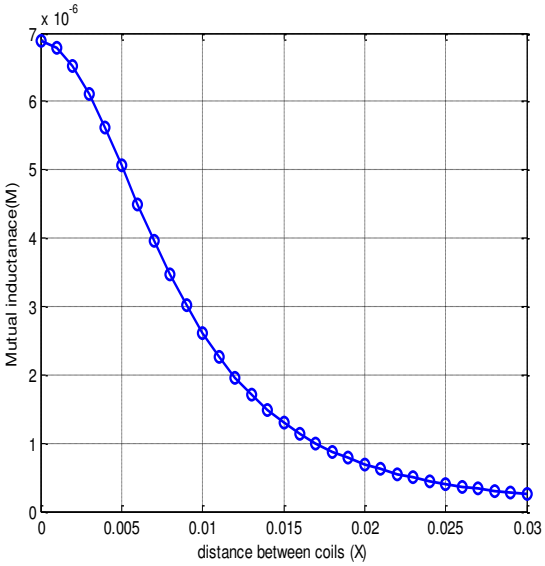

Figure-5. The relationship between distance and mutual inductance (M).

The spacing (s) between the turns also changes the efficiency value. The effect of the change in turn spacing from 0 mm to 1 mm for transmitter and receiver coil will effect in value of parasitic resistance as illustrated in Figure 6 (a) and (b) and that's lead to effect on efficiency as shown in figure 8 Based on the equation (17). As the turn spacing is increased, the parasitic resistance is increased. When the parasitic resistance is increased, the efficiency between the coils is decreased.

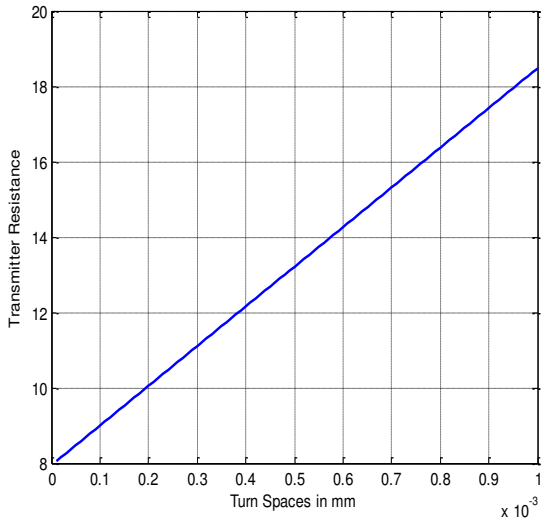

Figure-6. (a) Effect of variation of spacing (s) between the turn with change transmitter parasitic resistance.

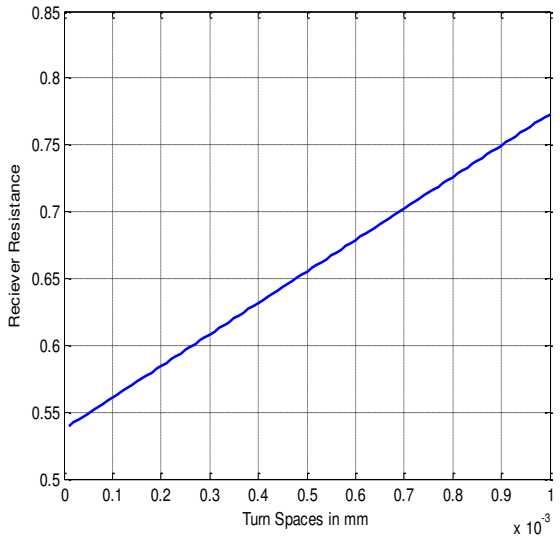

Figure-6. (b) Effect of variation of spacing (s) between the turn with change receiver parasitic resistance.

The width (W) of conductor turn also changes the efficiency value. The effect of the change in width turn from 0 mm to 1 mm for transmitter and receiver coil will effect in value of parasitic resistance as illustrated in Figure 7 (a) and (b) and that's lead to effect on efficiency as shown in Figure-8 Based on the equation (17). As the width turn is increased, the parasitic resistance is increased. When the parasitic resistance is increased, the efficiency between the coils is decreased.

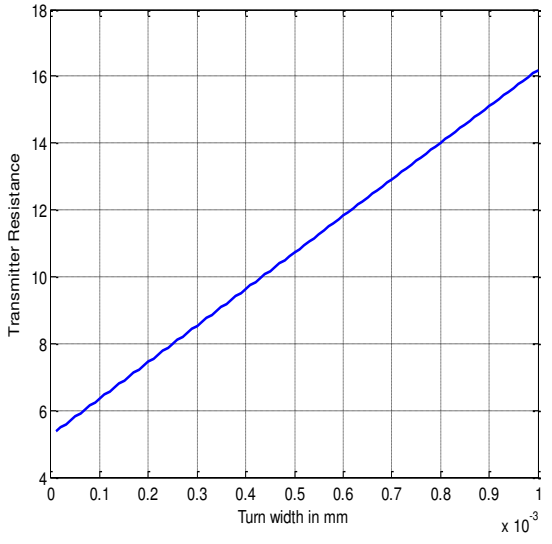

Figure-7. (a) Effect of variation of width turn (W) with change transmitter parasitic resistance.

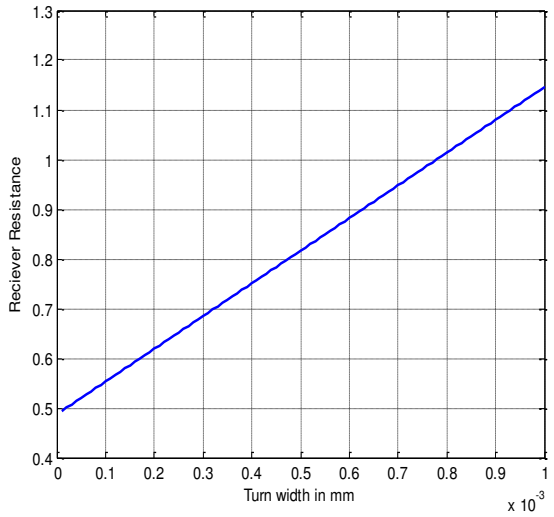

Figure-7. (b) Effect of variation of width turn (W) with change receiver parasitic resistance.

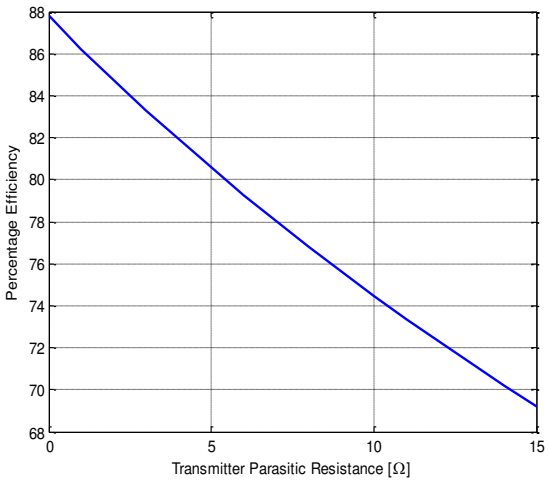

Figure-8. (a) Effect of variation of transmitter parasitic resistance with change efficiency.

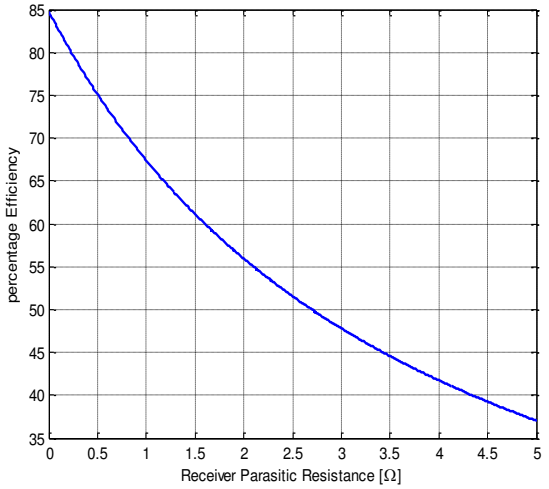

Figure-8. (b) Effect of variation of receiver parasitic resistance with change efficiency.

HFSS had been used as simulation environment for the implanted coil which has dimensions of: dout = 10.5 mm, din = 6.61 mm, n = 7, w = 0.14 mm and s = 0.137 mm and printed on a substrate (12 x 11.5 x 1.5) mm3. The antenna's gain was obtained on a sphere of radius 20 cm defined around the region of the antenna. An air box of dimensions (12 x 11.5 x 44) mm3 was defined as a radiation boundary using the algorithm of the FEM. The implanted antenna has an operating frequency of 6.78MHz.

The coil performance in the near-field is explained by plotting and analyzing, which comprises several resultant plots. This also involves the max near field, which displays the maximum radiated electric field in the near region, and the near E total, which is computed by the joint magnitude of the electric field components (i.e. Near E phi, Near E Theta, etc.). In near-field, the areas field components elevation and the azimuthal planes are not related to each other and can thus be plotted and observed separately. Figure 9 (a) and 9 (b) show the radiation patterns of the internal antenna on the elevation and the azimuthal planes at (0o and 90o) respectively.

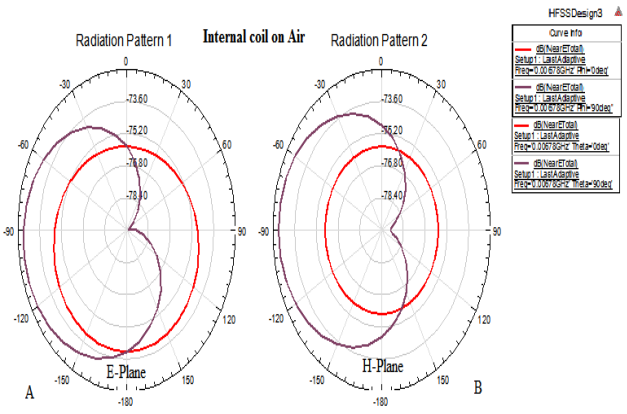

Figure-9. Simulated gain patterns of the implanted circular loop antenna on air: (A) Elevation Plane (Φ = 0o, Φ = 90o) and (B) Azimuthal Plane (θ = 0o, θ = 90o).

It can be seen that the gain in air is almost constant around the antenna and confirms the omnidirectional pattern associated with such loop antennas. The maximum gain surrounding coil is approximately -76 dB for both planes and there is a slight drop in the elevation plane at specific angles.

For deigning the external coil with dimensions of: dout = 44 mm, din = 7.92 mm, n = 27, w = 0.438 mm and s = 0.2 mm and printed on a substrate (50 x 46 x 1.5) mm3. The antenna gain was simulated on a sphere of radius 20 cm defined around the region of the antenna. The antenna has an operating frequency at 6.78 MHz, while other parameters were defined as in case of internal coil. The printed external coil performance is simulated on air, Figure 10 (a) and 10 (b) show the radiation patterns of the total antenna gain in the elevation and the azimuthal planes at (0o and 90o) respectively. The gain in air is also almost constant around the external coil and having

omnidirectional pattern. The maximum gain surrounding coil is approximately -51 dB for both planes and there is a slight change of azimuthal plane and slight drop in the elevation plane at specific angles.

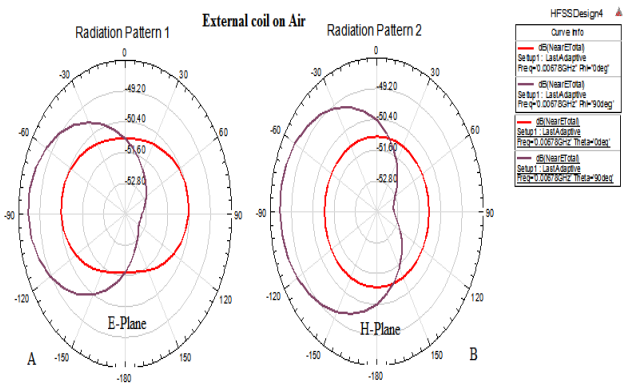

Figure-10. Simulated gain patterns of the external circular loop antenna on air: (a) Elevation Plane (Φ = 0o, Φ = 90o) and (b) Azimuthal Plane (θ = 0o, θ = 90o).

It can be seen that the gain in air is almost constant around the antenna and confirms the omnidirectional pattern associated with such loop antennas. The maximum gain surrounding coil is approximately -55.40 dB for both planes and there is a slight drop in the elevation plane at specific angles.

Table-2. Parameters and values for proposed inductive link.

Description	Symbol	Value
Primary inductance	L_T	16.95µH
Secondary inductance	L_R	0.654µH
Resistance primary	R_T	10.05 Ω
Resistance secondary	R_R	0.54Ω
Primary capacitance	C_T	39.18 PF
Secondary capacitance	C_R	827.17 PF
Primary Quality factor	Q_T	70.28
Secondary Quality factor	Q_R	51.56
Load resistance	R_{load}	200 Ω
Coefficient coupling	K	0.105
Mutual inductance	M	4.5 µH
Resonant frequency	f_0	6.78 MH_Z
Efficiency	η	74.47%
Distance	X	6 mm

To conclude the optimization of geometric coils design, Figure-11 shown the flow chart which describes the steps of coil design parameter.

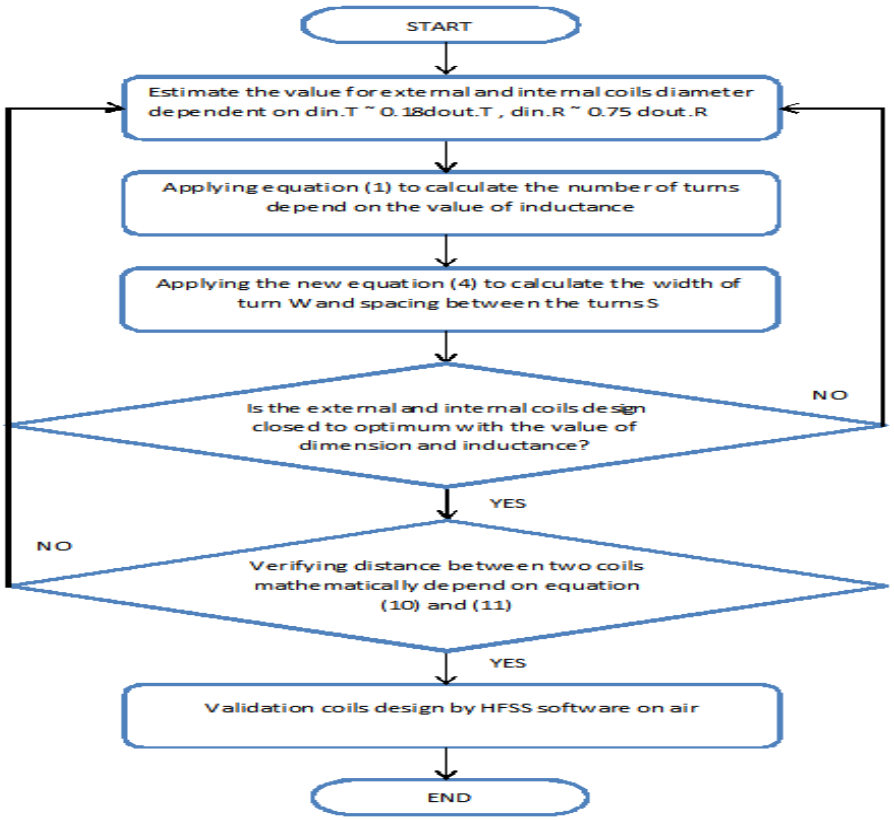

Figure-11. The flowchart of coil optimization parameters.

To verify the proposed coils, comparison with other designs was performed. The comparison included the coil shape, coils dimensions, operated frequency, radiated distance, modulation technique and applications. Table-3 shows that the proposed implanted spiral circular coil has smaller geometry values, larger distance transmission and feasibility.

Table-3. Comparison between the proposed coil design and other designs.

Coil shape	Tx-Coil (mm)	Rx-Coil (mm)	Carrier freq. (MHz)	Dist. (mm)	Modulation technique	Application	Ref.
circular	-	(5x8x2)	4	5	Downlink-ASK Uplink-LSK	Neural recording system	[16]
circular	50	20	4	28	-	EEG signal detection	[17]
Tx-solenoid Rx-Cylinder	d_{in}= 410 L= 300	10x13	1	205	-	endoscopy	[18]
Spiral pancake	d_{out}=52 d_{in}= 10	d_{out}=10 d_{in}= 5	6.78	10	ASK	brine	[11]
Tx-spiral coil Rx-rectangular	d_{out}=44	4x8	13.56	40	LSK	Subcutaneous tissue	[19]
square	(2x2) cm^2	(2x2) mm^2	915	15	_		[20]
Spiral rectangular	62x25	25x10	13.56	10	ASK	Implanted micro-system	[4]
Spiral square	70x8	20x8	1-5	10	ASK	--	[5]
circular	d_{out}=38 d_{in}= 36	d_{out}=18 d_{in}= 16	742 KHz	10	_	Neural recording system	[6]
Spiral circular	d_{out}=56 d_{in}= 10	d_{out}=11.6 d_{in}= 5	13.56	22	ASK	Nerves and muscles stimulator	[7]
Spiral rectangular	d_{out}=80 d_{in}=20	d_{out}=20 d_{in}=11	13.56	28	_	_	[21]
Spiral circular	d_{out}=44 d_{in}= 7.92	d_{out}=10.5 d_{in}= 6.61	6.78	15	ASK	Nerves and muscles stimulator	Prop osed

CONCLUSIONS

This paper developed an iterative design procedure that optimizes the design of a pair of printed spiral coils present in implantable microelectronic devices to maximize the inductive power transmission efficiency among them to reach up to 74.47%. Moreover, this procedure exhibits how power efficiency changes when different coil geometrical parameters vary in an extensive range. The optimizing conductor width and spacing between the turn of the primary coil followed the same between the turn in the secondary coil. This repetition goes on until the power efficiency attains its highest level for the chosen operating frequency at 6.78MHz ISM band and the coil relative distance. The finite element analysis models in HFSS using the optimal geometries are constructed. The recommended implanted coil is small and executes well, making it quite appropriate for implanting in micro-systems.

REFERENCES

[1] D. E. Johnson. 2006. Basic Electric Circuit Analysis: John Wiley and amp; Sons, Inc.

[2] S. Atluri and M. Ghovanloo. 2006. A wideband power-efficient inductive wireless link for implantable microelectronic devices using multiple carriers. in Circuits and Systems, 2006. ISCAS 2006. Proceedings. 2006 IEEE International Symposium on. p. 4, p. 1134.

[3] G. B. Hmida, M. Dhieb, H. Ghariani and M. Samet. 2006. Transcutaneous power and high data rate transmission for biomedical implants. In: Design and Test of Integrated Systems in Nanoscale Technology, 2006. DTIS 2006. International Conference on. pp. 374-378.

[4] L. Andia, R. F. Xue, C. Kuang-Wei, and J. Minkyu. 2011. Closed loop wireless power transmission for implantable medical devices. In: Integrated Circuits (ISIC), 2011 13th International Symposium on. pp. 404-407.

[5] M. Zargham and P. G. Gulak. 2012. Maximum Achievable Efficiency in Near-Field Coupled Power-Transfer Systems. Biomedical Circuits and Systems, IEEE Transactions on. 6: 228-245.

[6] X. Li, H. Zhang, F. Peng, Y. Li, T. Yang, B. Wang, et al. 2012. A wireless magnetic resonance energy transfer system for micro implantable medical sensors. Sensors. 12: 10292-10308.

[7] S. Mutashar, M. A. Hannan, S. A. Samad, and A. Hussain. 2014. Analysis and Optimization of Spiral Circular Inductive Coupling Link for Bio-Implanted Applications on Air and within Human Tissue. Sensors. 14: 11522-11541.

[8] J. F. Drazan, A. Gunko, M. Dion, O. Abdoun, N. C. Cady, K. A. Connor, *et al*. 2014. Archimedean Spiral Pairs with no Electrical Connections as a Pas-sive Wireless Implantable Sensor.

[9] K. M. Silay, C. Dehollaini, and M. Declercq. 2008. Improvement of power efficiency of inductive links for implantable devices. in Research in Microelectronics and Electronics, 2008. PRIME 2008. Ph.D. pp. 229-232.

[10] S. S. Mohan, M. del Mar Hershenson, S. P. Boyd, and T. H. Lee. 1999. Simple accurate expressions for planar spiral inductances. Solid-State Circuits, IEEE Journal of. 34: 1419-1424.

[11] R. R. Harrison. 2007. Designing Efficient Inductive Power Links for Implantable Devices. In: Circuits and Systems, 2007. ISCAS 2007. IEEE International Symposium on. pp. 2080-2083.

[12] M. Soma, D. C. Galbraith, and R. L. White. 1987. Radio-frequency coils in implantable devices: misalignment analysis and design procedure. Biomedical Engineering, IEEE Transactions on. pp. 276-282.

[13] D. C. Galbraith, M. Soma and R. L. White. 1987. A wide-band efficient inductive transdennal power and data link with coupling insensitive gain. IEEE Transactions on Biomedical Engineering. 4: 265-275.

[14] J. Uei-Ming and M. Ghovanloo. 2007. Design and Optimization of Printed Spiral Coils for Efficient Transcutaneous Inductive Power Transmission. Biomedical Circuits and Systems, IEEE Transactions on. 1: 193-202.

[15] S. Mutashar Abbas, M. A. Hannan, S. A. Samad, and A. Hussain, "Design of spiral circular coils in wet and dry tissue for bio-implanted micro-system applications. Progress in Electromagnetics Research M. 32: 181-200.

[16] T. Akin, K. Najafi, and R. M. Bradley. 1998. A wireless implantable multichannel digital neural recording system for a micromachined sieve electrode. Solid-State Circuits, IEEE Journal of. 33: 109-118.

[17] C. Sauer, M. Stanacevic, G. Cauwenberghs and N. Thakor. 2005. Power harvesting and telemetry in CMOS for implanted devices. Circuits and Systems I: Regular Papers, IEEE Transactions on. 52: 2605-2613.

[18] B. Lenaerts and R. Puers. 2007. An inductive power link for a wireless endoscope. Biosensors and Bioelectronics. 22: 1390-1395.

[19] M. M. Ahmadi and G. A. Jullien. 2009. A wireless-implantable microsystem for continuous blood glucose monitoring. Biomedical Circuits and Systems, IEEE Transactions on. 3: 169-180.

[20] S. O'Driscoll, A. Poon, and T. H. Meng. 2009. A mm-sized implantable power receiver with adaptive link compensation. In: 2009 IEEE International Solid-State Circuits Conference-Digest of Technical Papers.

[21] S. Mehri, J. Ben HadjSlama, A. C. Ammari, and H. Rmili. 2014. Genetic algorithm based geometry optimization of inductively coupled printed spiral coils for remote powering of electronic implantable devices. In: Computer and Information Technology (GSCIT), 2014 Global Summit on. pp. 1-6.